Mem. S.A.It. Vol. 79, 128

Memorie della

Relativistic Fe Kα lines with SIMBOL-X

Jörn Wilms

Dr. Karl-Remeis-Sternwarte, Astronomisches Institut der Universität Erlangen-Nürnberg, Sternwartstr. 7, 96049 Bamberg, Germany

Abstract. I give an overview of observations of relativistically broadened Kα lines as observed with current X-ray satellites. Broad lines have now been seen in a variety of different active galaxies and also in Galactic sources. The profiles observed indicate that the accretion flow close to the black hole is very complex. Due to its high effective area and its broad band capabilities, SIMBOL-X will be ideally suited for observations of such lines.

1. Introduction

1.1. Accretion in Active Galactic Nuclei

The broad-band spectra of Active Galactic Nuclei (AGN) can be well described as the sum of several distinct components: in the soft X-rays and the Ultra-Violet, a soft excess which is generally interpreted as thermal emission from an accretion disk with a temperature of a few 10 eV is seen, albeit often through a warm, ionized medium. At harder energies of a few keV, the spectra are power laws with a typical power law photon index of 1.7 to 1.9. As was shown, e.g., by Lightman & White (1988), the presence of a source of hard X-rays next to the colder, i.e., not fully ionized, accretion disk leads to a "Compton reflection hump", where hard X-rays are downscattered by multiple Thomson scatterings in the accretion disk, while softer X-rays from the source of the power law are absorbed in the disk. This Compton reflection hump is seen in many Seyfert galaxies and also in Galactic black holes.

The location of the source of hard X-rays is less clear. The prevailing opinion is that the hard X-rays are due to thermal Comptonization of soft photons from the accretion disk in a hot ($kT_\mathrm{e} \sim 100$ keV) electron plasma, which is situated close to the accretion disk (Haardt & Maraschi, 1993; Haardt et al., 1994). A possible geometry of such a configuration is depicted on the left panel of Fig. 1. Such an electron plasma could, e.g., be due to magnetic reconnection within the accretion disk, which is one of the possible mechanisms discussed as the source of the large viscosity of accretion disks (Balbus & Hawley, 1998). Note, however, that the plasma cannot fully cover the accretion disk, as the Compton cooling would be too strong (e.g., Dove et al., 1997). For this reason, it is generally assumed that the plasma forms either a "patchy corona" or that it is concentrated around the black hole in a quasi-spherical configuration. In recent years, mainly prompted by the discoveries of radio jets around Galactic black holes, which are thought to be very similar to AGN, as well as by the correlations found between the radio and X-ray emission from Galactic black holes and AGN (Merloni et al., 2003; Gallo et al., 2003; Falcke et al., 2004), some authors have also discussed the possibility that the hard X-rays are due to emission from

Send offprint requests to: J. Wilms

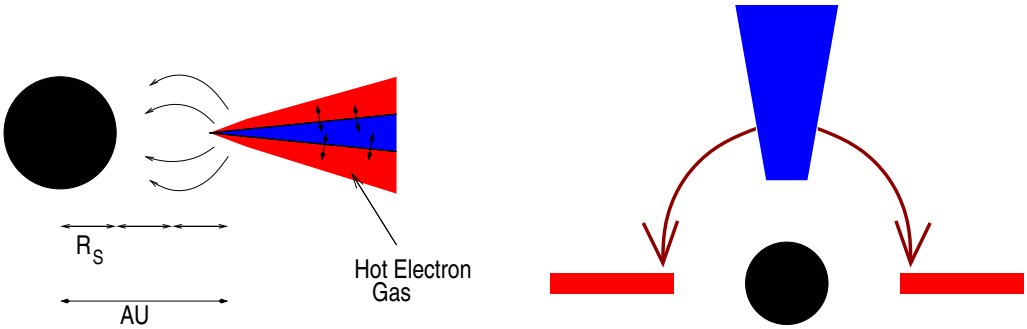

Fig. 1. The two accretion geometries posited for AGN. Left: A sandwiched "accretion disk corona", where a hot electron plasma surrounds the accretion disk. Right: The "lamppost model", where hard X-rays from the base of a jet irradiate the inner parts of the accretion disk.

the base of a radio jet (Markoff et al., 2005; Falcke et al., 2004). In this picture, shown on the right hand panel of Fig. 1, some of the hard X-rays are focused onto the accretion disk by the gravitational field of the black hole (Petrucci & Henri, 1997; Markoff & Nowak, 2004). A consequence of the absorption of hard X-rays in the accretion disk is the emission of strong fluorescent emission lines. Due to its high abundance and its high fluorescence yield, the most prominent of these lines is the Kα line of iron, emitted at 6.4–7 keV, depending on the ionization state of the disk. As these lines are emitted very close to the inner edge of the accretion disk, within only a few r_g from the black hole (where $r_g = GM/c^2$). Observations of fluorescent iron lines from AGN therefore provide the best diagnostics known today for studying the strong gravity close to supermassive black holes.

1.2. Relativistic iron lines

Early theoretical calculations of the radiative transfer in the accretion disk close to the black hole were performed, e.g., by Cunningham (1975). See Reynolds & Nowak (2003) for a recent review of the line properties and Dovčiak et al. (2004) and Brenneman & Reynolds (2006) for recent extensive calculations of line shapes under a variety of conditions. In the following I summarize their results.

Assuming Keplerian motion, the typical velocity of material close to the inner edge of the accretion disk is on the order of $0.4\,c$. Therefore, the observed iron line will be strongly Doppler broadened. The resulting line profile will have a typical double horned shape, with the lower energy ("red") horn being less strong than the blue horn, due to relativistic Doppler boosting. It is easy to see that the observed line profile will also depend on the inclination of the accretion disk, with edge on disks having the broadest line profiles as well as the gravitational redshift, as the line is emitted deep in the potential well of the black hole. Finally, the line profile will also be influenced by gravitational light bending (distant observers see the accretion disk behind the black hole due to space-time being distorted by the black hole).

The two most important parameters influencing the line shape, however, are the emissivity profile of the accretion disk and the angular momentum of the accretion disk. The emissivity profile, $\epsilon(r)$, is defined as the intensity of the emitted Fe Kα line per unit area of the disk. It is typically assumed to depend on the radial distance from the black hole. As the Fe Kα emissivity is proportional to the irradiated flux, the emissivity profile is geometry dependent. In the case of disks with sandwich accretion coronae, the emissivity profile traces the power released in the accretion disk as a function of the radius. If the hard radi-

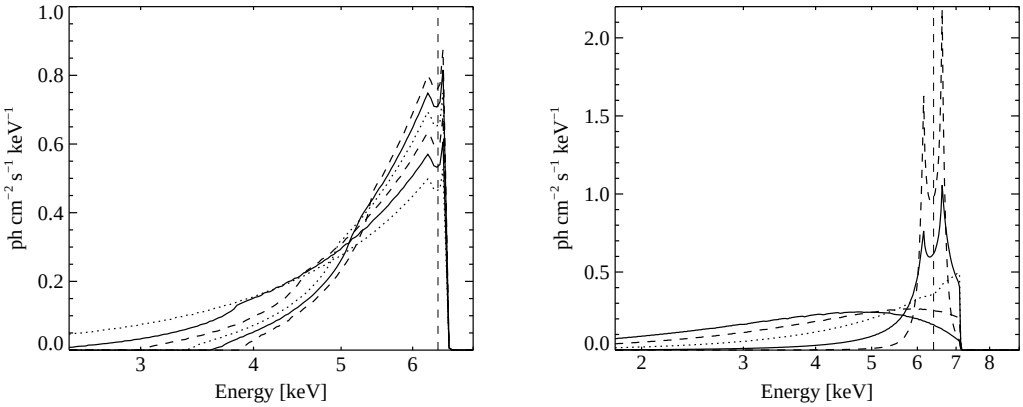

Fig. 2. Influence of the black hole spin and the emissivity profile onto the line profile (Wilms, 2005) *Left:* Broadening of the Fe Kα profile as a function of the black hole's angular momentum. The line profiles shown are computed for $a = 0.0$, 0.2, 0.4, 0.6, 0.8, and 0.998, and an inclination of 20° and a power-law disk emissivity of r^{-3} is assumed. *Right:* Influence of the disk emissivity profile, taken to be a power law of the form $\epsilon \propto r^{-\alpha}$, on the line shape, for $\alpha = 1$, 2, 3, 4, and 5. The more concentrated the emission is towards the inner edge of the disk, the broader the line. For both figures, a rest frame energy of 6.4 keV was assumed and the line profiles are normalized to a total line flux of 1 ph cm^{-2} s^{-1}. All line profiles have been computed using the code of Dovčiak et al. (Dovčiak et al., 2004), the thin dashed vertical line is at 6.4 keV.

ation comes from the base of a jet, on the other hand, then the emissivity profile depends on the distance of the source of hard X-rays from the black hole (Petrucci & Henri, 1997; Miniutti & Fabian, 2004). Often the emissivity is taken to be a (broken) power law. See the right hand panel of Fig. 2 for theoretical line profiles as a function of the steepness of the emissivity profile.

The second important parameter is the specific angular momentum of the black hole, $a = J/Mc$. As the inner edge of the accretion disk moves closer towards the black hole with increasing a, lines emitted close to maximally rotating Kerr black holes ($a = 0.998$) will be significantly broader than lines emitted from non-rotating Schwarzschild black holes ($a = 0$). This effect is illustrated in the left hand panel of Fig. 2. Lines from Kerr black holes can have red tails that extend to below 4 keV. Detecting such a tail is a direct evidence for black hole rotation. It is this dependence of the Fe Kα line on the spin that makes observations of the line so important: While the mass of the black hole can be inferred today with rather high precision, e.g., through the M-σ-relation (e.g., Gebhardt et al., 2000) or through maser observations (Miyoshi et al., 1995), as of today the only known way to measure the spin of a black hole is through analysis of the fluorescent Fe Kα line profile.

2. Previous observations of broad lines in AGN

After first tentative discoveries of broadened Fe Kα lines in Galactic black holes (Fabian et al., 1989), the first clear discovery of a relativistic line was made with *ASCA* in the Seyfert 1 galaxy MCG−6-30-15 (Tanaka et al., 1995). The line shape was found to be strongly flux dependent and, during a flux minimum state of the source, was shown to be so broad that MCG−6-30-15 must contain a Kerr black hole (Iwasawa et al., 1996). Subsequent studies, especially the observations with the X-ray CCDs on board XMM-Newton and Suzaku as well as the gratings on board Chandra confirmed this discovery. The signal to noise ratio of these recent observations is good enough to allow Brenneman & Reynolds (2006) to constrain the spin of the black hole in MCG−6-30-15 to $a = 0.989^{+0.009}_{-0.002}$, i.e., the black hole is maximally rotating. The ob-

servations of XMM-Newton during a deep minimum state show the emissivity profile to be $\propto r^{-4.6}$ (Wilms et al., 2001), while the line shape during a normal flux level can be well described by a line from a disk with a broken power law emissivity profile. In a 315 ksec long XMM-Newton observation, Fabian & Vaughan (2003) find $\epsilon \propto r^{-5.5}$ for $r < 6.6r_g$ and $\epsilon \propto r^{-2.7}$ for $r \geq 6.6r_g$, and later Suzaku observations find similar values (Miniutti et al., 2007). Such an emissivity profile is not explainable in the simple patched corona picture outlined above unless one invokes an additional source of energy close to the black hole (Wilms et al., 2001). Alternatively, as shown by Martocchia et al. (2002) the emissivity profile can be explained in the lamp-post model (Fig. 1, right panel), a result that is also consistent with the line and continuum variability (Miniutti et al., 2003). It should be stressed, however, that if this interpretation is true, then the canonical interpretation of the hard spectral component in Seyfert galaxies as being due to thermal Comptonization has to be challenged. Since the discovery of the broad line in MCG−6-30-15, relativistic lines have been found in many sources. Recent surveys of XMM-Newton observations of AGN show that relativistic lines are present in 10–20% of all AGN (Guainazzi et al., 2006; Jiménez-Bailón et al., 2005), somewhat less than first thought from the ASCA results (Nandra et al., 1997, but see Lubiński & Zdziarski 2001). Relativistic lines are also clearly seen in most Galactic black holes (e.g., Miller et al., 2002; Wilms et al., 2006; Fritz et al., 2006), and the line shapes in these systems also seem to imply rotating black holes (e.g., Miller et al., 2004). For AGN, relativistic lines have now been seen even in very luminous objects such as the broad line radio-quiet quasar Q0056−363 (Porquet & Reeves, 2003; Matt et al., 2005), which is has a broad Fe Kα line with a FWHM of 24500 km s^{-1}. Relativistic lines have also been seen out to high redshifts. A broad line is seen in a source at $z = 1.146$ in the Chandra Deep Field North (Comastri et al., 2004). Streblyanska et al. (2005) find that the average Fe Kα profile of the Lockman hole AGN is also broad. Finally, in many sources the broad lines are strongly variable, which will clearly be a case for long and repeated observations of such systems with SIMBOL-X. For example, in the Seyfert 1 galaxy NGC 3516, Iwasawa et al. (2004) detected possible periodic changes in the red wing of the line, which they interpret to be due to emission from a rotating flare at a distance between $7r_g$ and $16r_g$ from the black hole, which is estimated to have a mass of $M \sim (1 \ldots 5) \times 10^7\, M_\odot$ (see, however, Turner et al. 2005). See Miller (2007) for a recent review of further results for both Galactic and extragalactic black holes, and Wilms (2005) for more discussions of XMM-Newton observations on broad Fe Kα lines.

3. Broad lines with SIMBOL-X

In order to use the full potential of the diagnostic capabilities of broad Fe Kα lines, it is necessary to use X-ray detectors which have a good (CCD level) energy resolution, which cover a broad energy range to allow a good measurement of the continuum of the source on both sides of the line, and which have a large collecting area. While the detectors on Chandra and XMM-Newton fulfill the first condition, due to the rapid decrease in effective area above 7 keV resp. 9 keV, it is difficult to constrain the source continuum with these instruments. This has caused problems with the interpretation of some broad lines, e.g., in narrow line Seyfert galaxies, where both, strong relativistic lines and strong absorption edges, formally provide similar good fits to the data (e.g., Boller et al., 2003; Fabian et al., 2004). The XIS and HXD on Suzaku provide a broader spectral coverage, however, the small effective area of Suzaku makes observations of all but the brightest Seyfert galaxies uneconomically long.

SIMBOL-X clearly has none of these problems: it covers the large energy band required for the continuum determination and its low energy detectors have the resolution necessary to study the Fe Kα line profile. To gauge the expected quality of observations of broad lines with SIMBOL-X I have simulated a

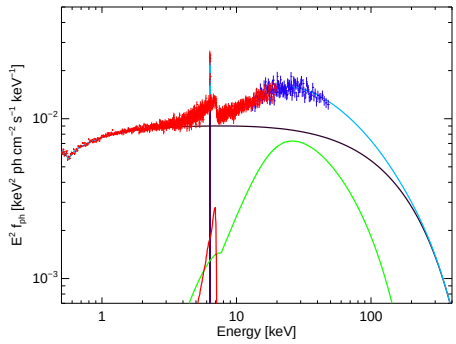

Fig. 3. Unfolded spectrum in (shown as a νf_ν-spectrum) of MCG−6-30-15 as seen with SIMBOL-X in a 100 ksec observation. Shown are the continuum spectrum, the narrow and the relativistic Fe Kα lines, and the relativistically smeared reflection continuum.

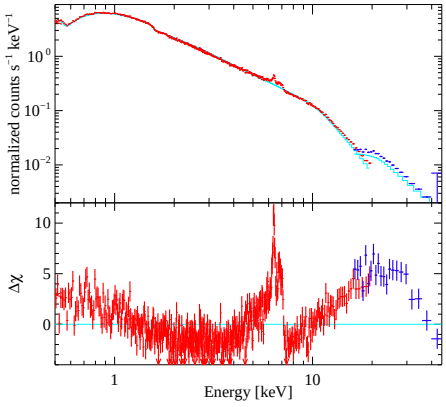

Fig. 4. Spectrum and residuals of a simulated 100 ksec SIMBOL-X observation of MCG−6-30-15. See text for further discussions.

100 ksec long observation of MCG−6-30-15. The spectral shape assumed in these simulations is a Comptonization continuum from a gas with $kT_e = 71$ keV and an optical depth of $\tau_e = 0.37$. The 2–10 keV continuum flux is $F_{2-10\,\mathrm{keV}} = 2.6 \times 10^{-11}$ cgs. Overlaid to the continuum is a narrow Fe Kα line, e.g., from the torus at an energy of $E = 6.4$ keV, with a width of $\sigma = 0.01$ keV and an equivalent width of EW = 52 eV, as well as a broad Fe Kα line from ionized iron (rest frame energy $E = 6.97$ keV) with an equivalent width of 500 eV, seen under an inclination of $i = 40°$. The line was assumed to come from a disk around a Kerr black hole ($R_{in} = 1.2GM/c^2$, $R_{out} = 400GM/c^2$) with an emissivity profile $\epsilon(r) \propto r^{-3}$. In addition, a relativistically smeared reflection continuum with a covering factor of $\Omega/2\pi = 1.5$ is present in the simulations. Figure 3 displays these components and the unfolded simulated data. Fitting the combined SIMBOL-X spectrum from the 100 ksec observation, excluding the 4–9 keV band, as shown in Fig. 4 both the Fe Kα line (including its non-Gaussian shape) and the Compton reflection hump are readily apparent and a determination of the spectral parameters used in the simulations is trivial. Going to a shorter exposure time of 10 ksec to gauge the capability of SIMBOL-X to determine short term variations of the line, I find that the following best-fit parameters: $\beta = 2.71^{+0.7}_{-0.4}$, $E = 6.6 \pm 0.1$ keV, and $i = 37^{+5.6}_{-4.8}$ deg. These results are significantly better than those obtainable with XMM-Newton ($\beta = 3.93^{+2.2}_{-0.7}$, $E = 6.5^{+1.1}_{-0.9}$ keV, and $i = 41 \pm 40$ deg). The main reason for this significant improvement expected with SIMBOL-X compared to current missions is the satellite's high energy capability. To summarize, in this contribution I have reviewed the diagnostic potential of relativistically broadened Fe Kα lines and recent observational results. We are now at a very exciting place in time, with current observations already starting to allow us to measure, for the first time, the spin of black holes by studying the broad lines. I have shown that such lines are seen in a significant number of Galactic and extragalactic sources. The simulations presented above predict that due to its broad band capabilities and the good energy resolution of the instruments on SIMBOL-X, this satellite will allow us to make further progress in understanding the broad lines of Active Galactic Nuclei.

Acknowledgements. It is a pleasure to acknowledge useful discussions with C.S. Reynolds, M.A. Nowak, K. Pottschmidt, M. Hanke, S. Fritz, and A.C. Fabian on the subject of this contribution. I acknowledge the support from the Deutsches Zentrum für Luft- und Raumfahrt (DLR).

References

Balbus, S. A. & Hawley, J. F. 1998, Rev. Mod. Phys., 70, 1

Boller, T., Tanaka, Y., Fabian, A., et al. 2003, MNRAS, 343, L89

Brenneman, L. W. & Reynolds, C. S. 2006, ApJ, 652, 1028

Comastri, A., Brusa, M., & Civano, F. 2004, MNRAS, 351, L9

Cunningham, C. T. 1975, ApJ, 202, 788

Dove, J. B., Wilms, J., Maisack, M. G., & Begelman, M. C. 1997, ApJ, 487, 759

Dovčiak, M., Karas, V., & Yaqoob, T. 2004, ApJS, 153, 205

Fabian, A. C., Miniutti, G., Gallo, L., et al. 2004, MNRAS, 353, 1071

Fabian, A. C., Rees, M. J., Stella, L., & White, N. 1989, MNRAS, 238, 729

Fabian, A. C. & Vaughan, S. 2003, MNRAS, 340, L28

Falcke, H., Körding, E., & Markoff, S. 2004, A&A, 414, 895

Fritz, S., Wilms, J., Pottschmidt, K., et al. 2006, in Proc. X-ray Universe 2005, ed. A. Wilson, ESA SP-604 (Noordwijk: ESA Publications Division), 267–268

Gallo, E., Fender, R. P., & Pooley, G. G. 2003, MNRAS, 344, 60

Gebhardt, K., Bender, R., Bower, G., et al. 2000, ApJ, 539, L13, erratum: ApJ 555, L75

Guainazzi, M., Bianchi, S., & Dovčiak, M. 2006, Astron. Nachr., 327, 1032

Haardt, F. & Maraschi, L. 1993, ApJ, 413, 507

Haardt, F., Maraschi, L., & Ghisellini, G. 1994, ApJ, 432, L95

Iwasawa, K., Fabian, A. C., Reynolds, C. S., et al. 1996, MNRAS, 282, 1038

Iwasawa, K., Miniutti, G., & Fabian, A. C. 2004, MNRAS, 355, 1073

Jiménez-Bailón, E., Piconcelli, E., Guainazzi, M., et al. 2005, A&A, 435, 449

Lightman, A. P. & White, T. R. 1988, ApJ, 335, 57

Lubiński, P. & Zdziarski, A. A. 2001, MNRAS, 323, L37

Markoff, S. & Nowak, M. A. 2004, ApJ, 609, 972

Markoff, S., Nowak, M. A., & Wilms, J. 2005, ApJ, 635, 1203

Martocchia, A., Matt, G., & Karas, V. 2002, A&A, 383, L23

Matt, G., Porquet, D., Bianchi, S., et al. 2005, A&A, 435, 867

Merloni, A., Heinz, S., & di Matteo, T. 2003, MNRAS, 345, 1057

Miller, J. 2007, ARA&A, 45, 441

Miller, J. M., Fabian, A. C., Reynolds, C. S., et al. 2004, ApJ, 606, L131

Miller, J. M., Fabian, A. C., Wijnands, R., et al. 2002, ApJ, 578, 348

Miniutti, G. & Fabian, A. C. 2004, MNRAS, 349, 1435

Miniutti, G., Fabian, A. C., Anabuki, N., et al. 2007, PASJ, 59, 315

Miniutti, G., Fabian, A. C., Goyder, R., & Lasenby, A. N. 2003, MNRAS, 344, L22

Miyoshi, M., Moran, J., Herrnstein, J., et al. 1995, Nature, 373, 127

Nandra, K., George, I. M., Mushotzky, R. F., Turner, T. J., & Yaqoob, T. 1997, ApJ, 477, 602

Petrucci, P. O. & Henri, G. 1997, A&A, 326, 99

Porquet, D. & Reeves, J. N. 2003, A&A, 408, 119

Reynolds, C. S. & Nowak, M. A. 2003, Phys. Rep., 377, 389

Streblyanska, A., Hasinger, G., Finoguenov, A., et al. 2005, A&A, 432, 395

Tanaka, Y., Nandra, K., Fabian, A. C., et al. 1995, Nature, 375, 659

Turner, T. J., Kraemer, S. B., George, I. M., Reeves, J. N., & Bottorff, M. C. 2005, ApJ, 618, 155

Wilms, J. 2005, in Astrophysical Sources of High Energy Particles and Radiation, ed. T. Bulik, B. Rudak, & G. Madejski, AIP Conf. Proc. 801, 15

Wilms, J., Kendziorra, E., Nowak, M. A., et al. 2006, in Proc. X-ray Universe 2005, ed. A. Wilson, ESA SP-604 (Noordwijk: ESA Publications Division), 217

Wilms, J., Reynolds, C. S., Begelman, M. C., et al. 2001, MNRAS, 328, L27